The EMBO Journal (2011) 30, 2675–2689 | © 2011 European Molecular Biology Organization | All Rights Reserved 0261-4189/11
www.embojournal.org

THE EMBO JOURNAL

SCF^{FBXL15} regulates BMP signalling by directing the degradation of HECT-type ubiquitin ligase Smurf1

This article has been corrected and a corrigendum is also printed in this issue.

Yu Cui[1,4], Shan He[1,2,4], Cencan Xing[3,4], Kefeng Lu[1], Jian Wang[1], Guichun Xing[1], Anming Meng[3], Shunji Jia[3,*], Fuchu He[1,2,3,*] and Lingqiang Zhang[1,2,*]

[1]State Key Laboratory of Proteomics, Beijing Proteome Research Center, Beijing Institute of Radiation Medicine, Beijing, China, [2]College of Life Science and Bio-engineering, Beijing University of Technology, Beijing, China and [3]School of Life Sciences, Tsinghua University, Beijing, China

Smad ubiquitination regulatory factor 1 (Smurf1), an homologous to E6AP C-terminus (HECT)-type E3 ubiquitin ligase, performs a crucial role in the regulation of the bone morphogenetic protein (BMP) signalling pathway in both embryonic development and bone remodelling. How the stability and activity of Smurf1 are negatively regulated remains largely unclear. Here, we report that F-box and LRR domain-containing protein 15 (FBXL15), an F-box protein of the FBXL family, forms an Skp1-Cullin1-F-box protein-Roc1 $(SCF)^{FBXL15}$ ubiquitin ligase complex and targets Smurf1 for ubiquitination and proteasomal degradation. FBXL15, through its leucine-rich repeat domain, specifically recognizes the large subdomain within the N-lobe of the Smurf1 HECT domain and promotes the ubiquitination of Smurf1 on K355 and K357 within the WW-HECT linker region. In this way, FBXL15 positively regulates BMP signalling in mammalian cells. Knockdown of *fbxl15* expression in zebrafish embryos by specific antisense morpholinos causes embryonic dorsalization phenocoping BMP-deficient mutants. Injection of FBXL15 siRNAs into rat bone tissues leads to a significant loss of bone mass and decrease in bone mineral density. Collectively, our results demonstrate that Smurf1 stability is suppressed by SCF^{FBXL15}-mediated ubiquitination and that FBXL15 is a key regulator of BMP signalling during embryonic development and adult bone formation.

The EMBO Journal (2011) **30,** 2675–2689. doi:10.1038/emboj.2011.155; Published online 13 May 2011
Subject Categories: signal transduction; development

Keywords: bone remodelling; E3 ubiquitin ligase; embryonic development; SCF complex; Smad ubiquitination regulatory factor 1

*Corresponding authors. S Jia, Medical Building C126/C121, Tsinghua University, Beijing 100084, China. Tel.: +86 106 277 2435; Fax: +86 106 279 4401; E-mail: jiasj@mail.tsinghua.edu.cn or F He or L Zhang, State Key Laboratory of Proteomics, Beijing Proteome Research Center, Beijing Institute of Radiation Medicine, 27 Taiping Road, Beijing 100850, China. Tel.: +86 108 070 5115; Fax: +86 108 070 5115; E-mail: hefc@nic.bmi.ac.cn or Tel.: +86 106 817 7417; Fax: +86 106 817 7417; E-mail: zhanglq@nic.bmi.ac.cn
[4]These authors contributed equally to this work

Received: 27 January 2011; accepted: 20 April 2011; published online: 13 May 2011; corrected: 6 July 2011

Introduction

Protein ubiquitination is a highly ordered multi-step enzymatic cascade catalysed by ubiquitin-activating enzymes (E1s), ubiquitin-conjugating enzymes (E2s), and ubiquitin ligases (E3s) (Hershko and Ciechanover, 1998). E3 ubiquitin ligases are classified into the *r*eally *i*nteresting *n*ew *g*ene (RING) finger and *h*omologous to *E*6AP *c*arboxyl *t*erminus (HECT) domain categories (Rotin and Kumar, 2009). Smad ubiquitination regulatory factor 1 (Smurf1) and Smurf2 are close members of the HECT-type neural precursor cell-expressed developmentally downregulated gene 4 (Nedd4) family ligases with a C2-WW-HECT architecture, and they have critical roles in the regulation of the transforming growth factor β (TGF-β) and bone morphogenetic protein (BMP) signalling pathways (Zhu *et al*, 1999; Yamashita *et al*, 2005), as well as the Wnt (Narimatsu *et al*, 2009) and RhoA pathways (Wang *et al*, 2003). Smurf1 was originally identified as the E3 ligase of Smad1/5, and it dorsalizes ventral mesoderm and neuralizes ectoderm by modulating BMP signalling in *Xenopus* embryos (Zhu *et al*, 1999). Smurf1 also has a specific suppressing role in adult bone formation, but not in embryonic bone development or adult bone resorption (Zhao *et al*, 2003, 2010; Yamashita *et al*, 2005). $Smurf1^{-/-}$ mice exhibit an age-dependent increase in bone mass due to augmented BMP responses (Yamashita *et al*, 2005). Given the significant role of Smurf1 during embryonic development and adult bone homoeostasis maintenance, the stability and activity of Smurf1 should be tightly controlled.

We previously demonstrated that the PH domain-containing protein casein kinase 2-interacting protein 1 (CKIP-1) functions as an auxiliary factor to enhance Smurf1 activation through binding to the WW domains linker (Lu *et al*, 2008). $CKIP\text{-}1^{-/-}$ mice display an age-dependent bone mass increase due to decrease of Smurf1 activity (Lu *et al*, 2008). Regarding the negative regulation of Smurf1, a recent study showed that Smurf2 interacts with Smurf1 to induce the degradation of Smurf1, whereas Smurf1 failed to induce the degradation of Smurf2. Knockdown of Smurf2 in human breast cancer cells resulted in the enhancement of cell migration *in vitro* and bone metastasis *in vivo* (Fukunaga *et al*, 2008). Because the study was performed with a breast cancer cell line MDA-MB-231, the physiological role of Smurf1 regulation by Smurf2 under developmental conditions remains uncharacterized. To date, how Smurf1 is negatively regulated still remains unclear.

To search for more regulators of Smurf1, a yeast two-hybrid screening using Smurf1 as bait was performed (Li *et al*, 2010). One of the candidate interactors is the F-box protein: F-box and leucine-rich repeat (LRR) domain-containing protein 15 (FBXL15). F-box proteins are the variable substrate adaptors for the Skp1-Cullin1-F-box protein-Roc1 (SCF) ligase complexes, and they dictate the substrate specificity (Skaar *et al*, 2009a, b). The SCF ligases mediate the timely proteolysis of important eukaryotic cellular regulators and are involved in diverse cellular processes, including cell-cycle progression and tumourigenesis (Cardozo and Pagano, 2004). Cullin1 acts as the scaffold to recruit the Skp1-F-box protein pair to its N-terminus and Roc1 plus an E2 enzyme to its C-terminus (Skaar *et al*, 2009a). The F-box protein usually contains an N-terminal F-box, which mediates Skp1 binding and then is linked to the rest of the SCF complex, although not all F-box proteins form E3 complexes (e.g. FBXL10 and FBXL11). In addition, the F-box protein contains certain substrate-recognition modules, and based on this homology, they fall into three groups: FBXW subfamily with WD40 repeats, FBXL with LRR, and FBXO with other domains (Jin *et al*, 2004). There are a total of 69 human F-box proteins, but nearly 70% of them have not yet been matched with any substrates, a category that included the here identified FBXL15.

Here, we show that FBXL15 forms a functionally active SCF complex and targets Smurf1 for ubiquitination and proteasomal degradation. Importantly, we identify a critical role of FBXL15 in both the determination of dorsalization/ventralization during embryonic development and bone homoeostasis maintenance in the adult stage. So far as we know, this is the first evidence to show the physiological role of FBXL15 in BMP signalling and to indicate the negative regulatory mechanism of Smurf1 stability control.

Results

Identification of F-box protein FBXL15 as an Smurf1-interacting protein

A yeast two-hybrid screen was performed using the WW-HECT of human Smurf1 as bait, as the WW domains are responsible for substrate recognition, whereas the HECT is the catalytic domain (Rotin and Kumar, 2009). One of the recovered interactors encoded the full length of the F-box protein FBXL15 (Figure 1A). This prey attracted our interest for further investigation because most F-box proteins serve as substrate-recognition subunit of SCF ubiquitin ligases (Cardozo and Pagano, 2004). FBXL15 is highly conserved across species, with nearly 95% identity among mammals (Supplementary Figure S1A). Human FBXL15 contains an F-box domain (aa 22–64) in the N-terminus and six LRR repeats (aa 113–269) distributed in the resting regions (Figure 1A).

To ascertain whether the observed interaction was direct, the FBXL15-Smurf1 association was tested in an *in vitro* binding assay. GST-fused FBXL15 protein, but not GST alone, interacted with Smurf1 (Figure 1B). We then tested whether the interaction between the two proteins occurs in a physiological context. For this purpose, we first generated a specific antibody, which recognized both endogenous and ectopic FBXL15 protein and designed FBXL15-targeting siRNAs (Supplementary Figure S1B and C). The FBXL15 siRNA had no off-target effects on other F-box proteins (Supplementary Figure S1D). Using this antibody, we observed that FBXL15 was widely expressed in mouse heart, liver, spleen, bone, muscle, brain, and kidney, as well as in various human cell lines (Supplementary Figure S1E and F). Importantly, an immunoprecipitate of endogenous Smurf1 contained significant amounts of FBXL15, whereas a pre-immune IgG failed to immunoprecipitate any FBXL15 (Figure 1C). FBXL15 interacted with wild-type Smurf1 and the ligase-inactive C699A mutant to similar extents (Figure 1D). FBXL15 and Smurf1 were colocalized in the cytoplasm (Figure 1E; Supplementary Figure S1G). Together, these data demonstrate that FBXL15 interacts with Smurf1 both *in vitro* and endogenously in cultured cells.

Deletion analysis revealed that the LRR domains of FBXL15 and the HECT domain of Smurf1 were both sufficient and necessary for the interaction (Figure 1F and G). The HECT domain is the catalytic region of Smurf1 and consists of two lobes: an N-terminal lobe and a C-terminal lobe. The N-terminal lobe consists of a large and a small subdomain. The small subdomain of the N-lobe contains the E2-binding site, whereas the C-lobe contains the catalytic cysteine (C699), which forms a thioester intermediate with ubiquitin (Rotin and Kumar, 2009). In contrast, the role of the large subdomain remains less well known. Interestingly, the large subdomain of Smurf1 was both required and sufficient for interaction with FBXL15 (Figure 1H and I). Thus, the LRR domains of FBXL15 and the HECT large subdomain of Smurf1 mediate their interaction.

SCF^{FBXL15} targets Smurf1 for proteasomal degradation

LRR domains of FBXL family are usually responsible for substrate recognition (Skaar *et al*, 2009a). The fact that the

Figure 1 Smurf1 interacts with FBXL15 both *in vitro* and in cultured cells. (**A**) The 'bait' and the 'prey' regions of Smurf1 and FBXL15 in yeast two-hybrid screening are shown schematically. (**B**) Direct interaction between FBXL15 and Smurf1 was revealed by GST pull-down assays. Both input and pull-down samples were subjected to immunoblotting with anti-His and anti-GST antibodies. Input represents 20% of that used for pull down. (**C**) Co-immunoprecipitation (Co-IP) of endogenous FBXL15 and endogenous Smurf1 from HEK293 cells. Western-blot analysis of whole-cell lysates and immunoprecipitates with Smurf1 antibody or control IgG. To avoid Smurf1 degradation, the proteasome inhibitor MG132 was added and incubated for 12 h before the cells were harvested. IP, immunoprecipitate; IB, immunoblotting; IgG, immunoglobulin; IgG HC, IgG heavy chain. (**D**) FBXL15 was co-immunoprecipitated with both wild type and catalytic mutant forms of Smurf1. HEK293T cells transfected with Myc-FBXL15 and Flag-Smurf1 (WT or C699A) were immunoprecipitated with anti-Flag, followed by immunoblotting analysis. (**E**) FBXL15 was colocalized with Smurf1 within the cytoplasm. Myc-FBXL15 and Flag-Smurf1 were cotransfected into MCF7 cells and 24 h later stained with mouse anti-Flag and rabbit anti-Myc antibodies before visualization by confocal microscopy. To avoid Smurf1 degradation, MG132 was added and incubated for 12 h before the cells were harvested. (**F**) FBXL15 interacts with Smurf1 through its LRR domains. Flag-Smurf1 and FBXL15 deletion mutants were transfected into HEK293T cells, and Co-IP assays were performed. Asterisks indicate FBXL15 deletion mutants. (**G**, **H**) Mapping of interacting regions of Smurf1 with FBXL15. Flag-FBXL15 and the indicated Smurf1 truncates were coexpressed in HEK293T cells. Cell lysates were incubated with anti-Flag to precipitate Smurf1 deletion mutants. Both the lysates and the immunoprecipitates were analysed by western blot with the indicated antibodies. Asterisks indicate Smurf1 deletion mutants. HECT-N-lobe-L/S, the large/small subdomain of Smurf1 HECT N-lobe. (**I**) Schematic representation of the binding regions between Smurf1 and FBXL15.

LRR of FBXL15 mediates the interaction with Smurf1 led us to investigate whether Smurf1 is the substrate of SCF^{FBXL15}. Considering that not all F-box proteins form E3 ligase complexes with Cullin1 and Roc1, we first examined the interaction of FBXL15 with common SCF subunits in mammalian cells. As shown in Figure 2A, FBXL15 could be co-immunoprecipitated with endogenous Cullin1, Skp1, and Roc1, but the ΔF mutant could not be, indicating that it does indeed form a genuine and typical SCF complex. Coexpression of FBXL15 with Smurf1 resulted in a significant decrease in the Smurf1 protein level, whose effect was blocked by treatment with the proteasome inhibitor MG132 (Figure 2B; Supple-

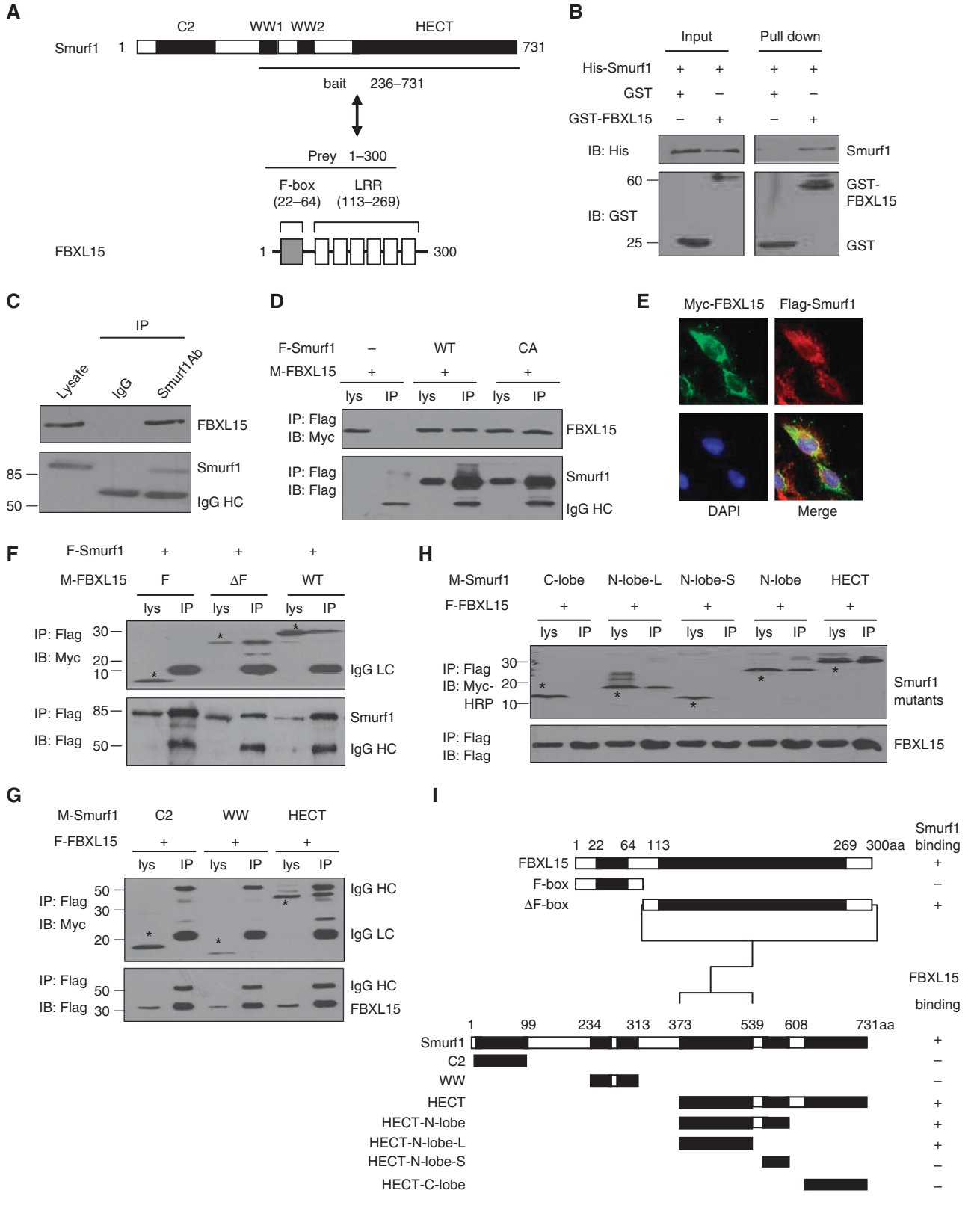

mentary Figure S2A). Remarkably, FBXL15 downregulated the stability of both the Smurf1 WT and C699A, ruling out the possibility that FBXL15 promotes Smurf1 degradation by augmenting the Smurf1 *cis*-E3 activity. Additionally, neither the F-box nor the ΔF truncates of FBXL15 had any significant effects on Smurf1 levels (Figure 2C), indicating that both the direct interaction between FBXL15 and Smurf1 mediated by the LRR and the intact SCF complex mediated by the F-box are

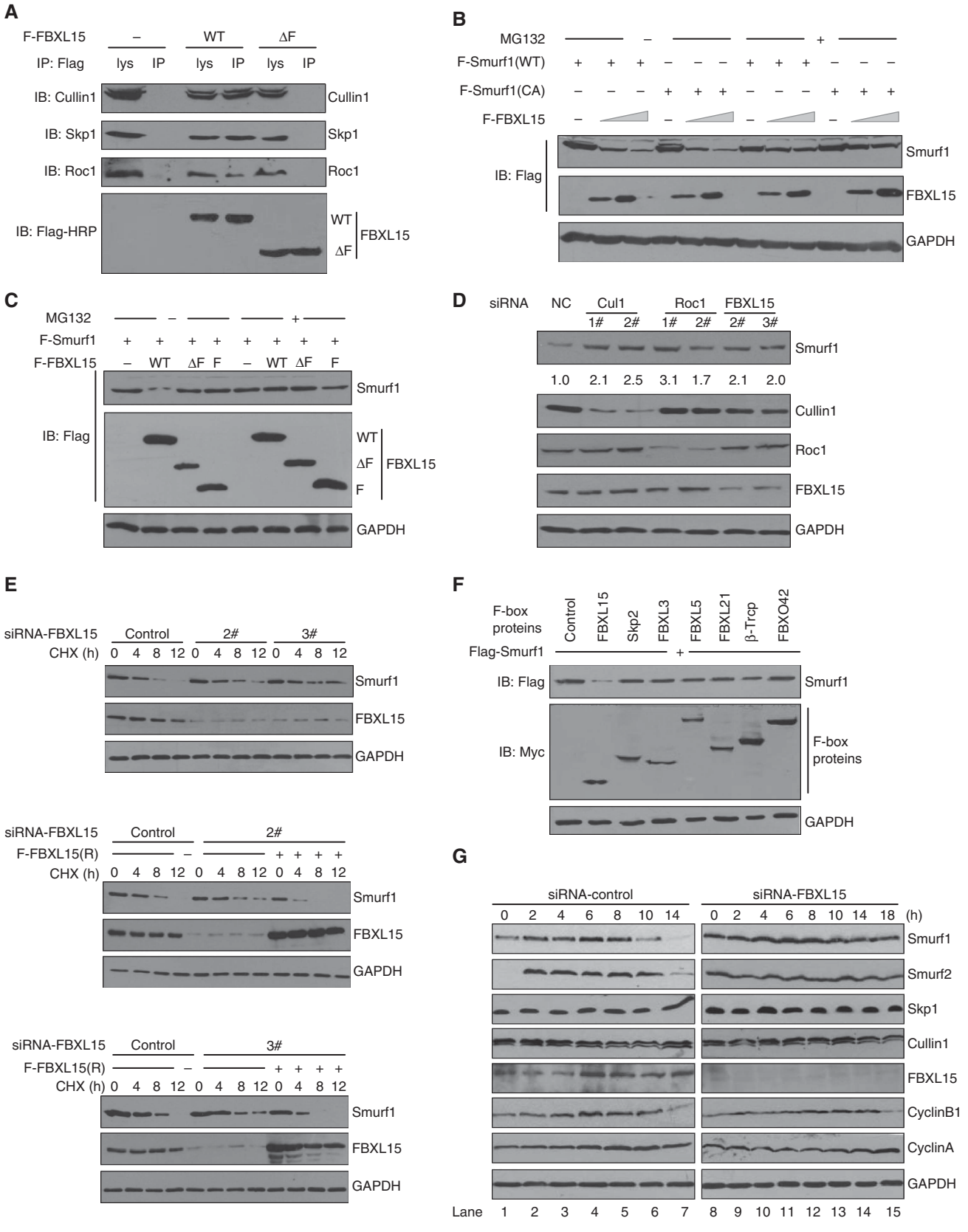

required for FBXL15 to efficiently regulate Smurf1. In contrast, overexpression of Smurf1 had no significant effect on the protein level of FBXL15 (Supplementary Figure S2B).

Next, we asked whether endogenous SCF^{FBXL15} affects the Smurf1 protein. To this end, FBXL15, Cullin1, or Roc1 was each depleted by two independent siRNA duplexes in HEK293T cells. We observed a 1.7–2.5-fold increase in the Smurf1 protein level in cells depleted of FBXL15, Cullin1, or Roc1 relative to control cells (Figure 2D). Furthermore, the half-life of endogenous Smurf1 was approximately 6 h in control cells and it was greatly increased to >9 h after depletion of FBXL15 (Figure 2E, top panels; Supplementary Figure S2C). Introduction of the siRNA-resistant FBXL15 mutant reversed the effects of FBXL15 siRNA and resulted in accelerated degradation of Smurf1 (Figure 2E, middle and bottom panels). Importantly, the regulation of Smurf1 by FBXL15 was specific. Indeed, overexpression of six other F-box proteins did not affect Smurf1 levels (Figure 2F). Thus, endogenous FBXL15 causes the destabilization of endogenous Smurf1 protein.

The SCF complex has been shown to have a role in controlling cell-cycle progress. We next tested whether the stability of Smurf1 has any cell-cycle dependence. The results indicated that Smurf1 (and Smurf2) were upregulated when the cells entered into S and G2 phases (2–8 h after thymidine-aphidicolin release) (Figure 2G, lanes 2–5). At the later stage of G2 phase (10 h) and the M phase (14 h), FBXL15 were upregulated, companied by a significant decrease of Smurf1/2 levels (lanes 6–7). In contrast, the expression of Cullin1 and Roc1 remains constant during this process. Importantly, in the FBXL15-depleted cells, the levels of Smurf1 (and Smurf2) were constant within the 18 h after thymidine-aphidicolin release (lanes 8–15). These results suggested that SCF^{FBXL15} might have a role in the G2/M progression at least partially through targeting Smurf1 (and Smurf2) for degradation.

SCF^{FBXL15} promotes the ubiquitination of Smurf1

As most F-box proteins involve the substrate's turnover by ubiquitination, we sought to determine whether FBXL15-mediated Smurf1 degradation is a consequence of ubiquitination. As shown in Figure 3A, in the absence of ectopic FBXL15, the ubiquitination of Smurf1 WT (lane 2) and CA (lane 4) can be both detected. The latter was less than the former and should be mediated by endogenous FBXL15. FBXL15 overexpression strongly enhanced the ubiquitination of Smurf1 (lanes 3 and 5). Knockdown of endogenous FBXL15 or Cullin1 or Roc1 resulted in decrease of Smurf1 ubiquitination (Figure 3B), indicating SCF^{FBXL15} indeed functions as E3 ligase of Smurf1 in cultured cells.

The E2 used by FBXL15 being unknown, we tested two proteins that are frequently used by mammalian RING finger E3s: UbcH5c and UbcH7. Incubation with FBXL15 purified from cultured cells, in the presence of either UbcH5c or UbcH7, led to the ubiquitination of His-Smurf1 (Figure 3C). To further evaluate the capacity of FBXL15 to directly ubiquitinate Smurf1, we carried out the ubiquitination of Smurf1 *in vitro* using a semi-purified system. Bacteria-expressed and purified Smurf1 ligase could catalyse the auto-ubiquitination in the presence of HA-Ub and E1/E2/ATP (Figure 3D, lane 2). Incubation of this mixture with purified GST-FBXL15 protein alone or GST/Cul1/Roc1/Skp1 elution (the Cul1/Roc1/Skp1 were expressed as Myc-tagged proteins in HEK293T cells and the cell lysate was pull down by GSH beads) had no significant effects on the Smurf1 ubiquitination (lanes 3 and 4). Strikingly, incubation with GST-FBXL15/Cul1/Roc1/Skp1 (lane 5), but not the GST-FBXL15-ΔF/Cul1/Roc1/Skp1 complex (lane 6), resulted in a dramatic increase of Smurf1 ubiquitination, indicating that an intact SCF complex was both sufficient and required for promoting the Smurf1 ubiquitination. Again, this ubiquitination was independent of Smurf1 ligase activity since Smurf1-C699A was effectively ubiquitinated by GST-FBXL15/Cul1/Roc1/Skp1 (lane 9), whose effect also required the entire SCF complex (lanes 8 and 10). Notably, FBXL15 seems not to function as an adaptor to change the structure of Smurf1 for its auto-ubiquitination since incubation with GST alone or GST-FBXL15 protein had no significant effects on Smurf1 auto-ubiquitination under the *in vitro* ubiquitination conditions (Figure 3E, lanes 3 and 4). As a positive control, incubation with the Smurf1 cofactor CKIP-1 (Lu *et al*, 2008) resulted in a dramatic increase of Smurf1 auto-ubiquitination *in vitro* (lane 5). In addition, Smurf2 depletion in HEK293T cells had no significant effect on the FBXL15 activity of regulating Smurf1 ubiquitination (Supplementary Figure S3), implicating that FBXL15 might regulate Smurf1 ubiquitination in an Smurf2-independent manner. Collectively, these data demonstrate that SCF^{FBXL15} complex is a bona fide E3 ligase for Smurf1.

Lysines 355 and 357 of Smurf1 are major ubiquitination sites for FBXL15

As the HECT domain is essential for Smurf1 association with FBXL15, we asked whether HECT domain alone is sufficient

Figure 2 FBXL15 forms a functionally active SCF complex and promotes the proteasomal degradation of Smurf1. (**A**) FBXL15 is associated with Skp1, Cullin1, and Roc1. HEK293T cells transfected with empty vector, Flag-FBXL15 or Flag-FBXL15-ΔF were immunoprecipitated with anti-Flag, and then whole-cell lysates and immunoprecipitates were subjected to immunoblotting with anti-Cullin1, anti-Skp1, and anti-Roc1 antibodies. (**B**) FBXL15 expression decreases the steady-state level of Smurf1 WT and C699A mutant. HEK293T cells were transfected with a constant amount of Smurf1 (WT or CA) and increasing amounts of FBXL15. After 24 h, cells were treated with MG132. Aliquots of total lysates were immunoblotted to detect Smurf1 and FBXL15. (**C**) Wild-type FBXL15, but not FBXL15 deletions, promote Smurf1 degradation. HEK293T cells were transfected with Flag-Smurf1 and various FBXL15 mutants. Cells were treated with or without MG132 for 12 h and harvested to detect Smurf1. (**D**) Knockdown of Cullin1, Roc1, or FBXL15 stabilizes endogenous Smurf1. HEK293T cells were transfected with two independent siRNA duplexes against Cullin1 (1# and 2#), Roc1 (1# and 2#), FBXL15 (2# and 3#), or non-targeting control siRNA. Cell lysates were analysed by immunoblotting with the indicated antibodies. Relative intensity of the Smurf1 bands is indicated. (**E**) Knockdown of FBXL15 increases the half-life of endogenous Smurf1. HEK293T cells were transfected with control siRNA, 2# or 3# siRNAs against FBXL15 or cotransfected with FBXL15 siRNA-resistant mutants. Thirty-six hours after transfection, cells were treated with cycloheximide (50 μg/ml) for the indicated times and then harvested for immunoblotting. (**F**) Smurf1 degradation is specific to FBXL15. HEK293T cells were transfected with the indicated Myc-tagged F-box protein constructs together with Flag-Smurf1. Cell lysates were harvested and analysed by immunoblotting. (**G**) HeLa cells transfected with control siRNA or FBXL15 siRNA were synchronized by thymidine-aphidicolin (2 mM) treatment. At the indicated time after release, the indicated proteins were analysed by immunoblotting.

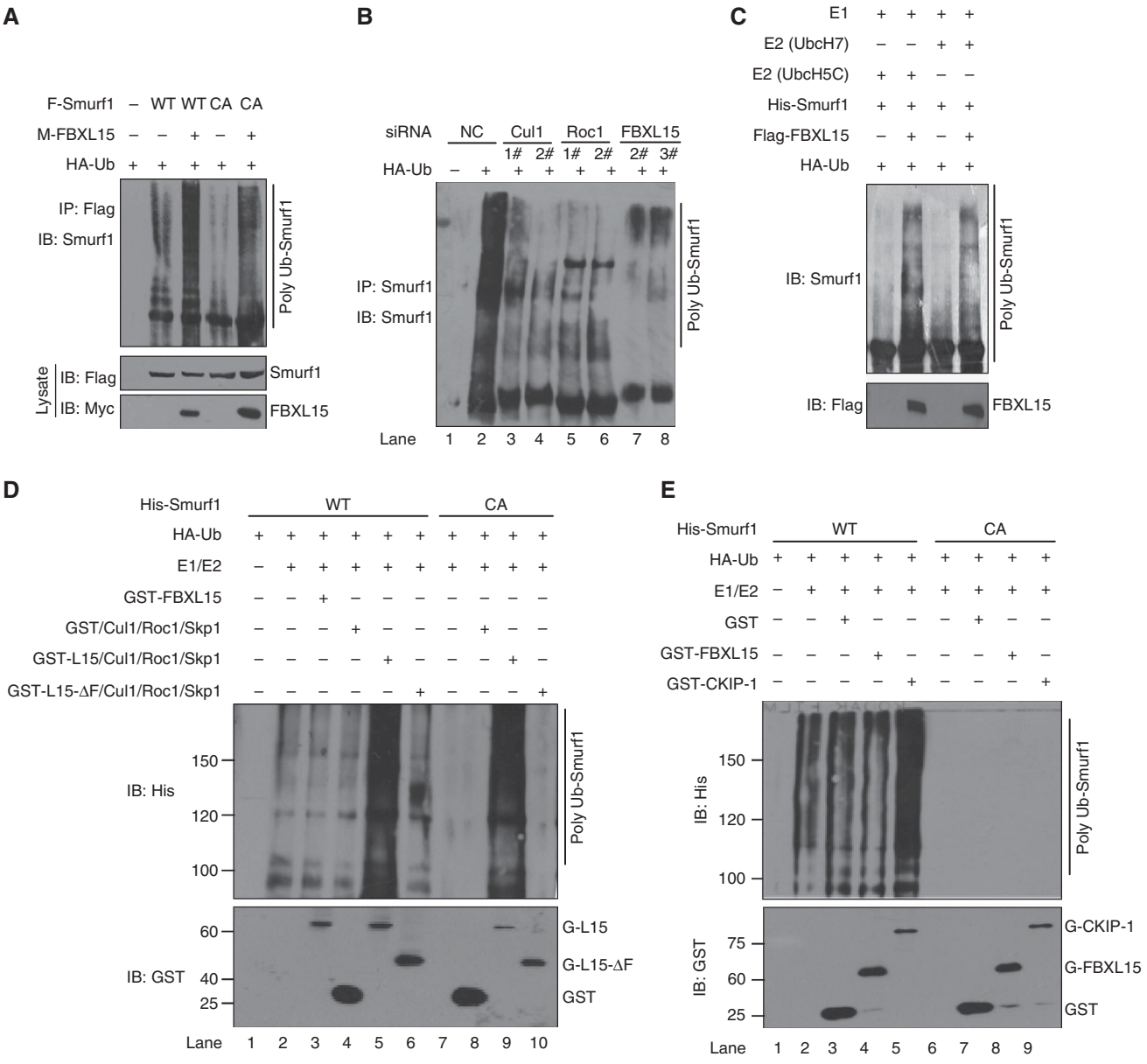

Figure 3 FBXL15 promotes Smurf1 ubiquitination. (**A**) FBXL15 promotes Smurf1 ubiquitination *in vivo*. HEK293T cells were cotransfected with Flag-Smurf1 (WT or CA) and HA-Ub, with or without Myc-FBXL15. Ubiquitinated Smurf1 were immunoprecipitated with an anti-Flag antibody and protein A/G-agarose beads under denaturing conditions to eliminate any Smurf1-associated proteins through non-covalent bonds. (**B**) Knockdown of endogenous Cullin1, Roc1, or FBXL15 decreased Smurf1 ubiquitination. HEK293T cells were transfected with indicated siRNAs and HA-Ub. Smurf1 ubiquitination were immunoprecipitated and detected with Smurf1 antibody. (**C**) To determine the efficiency of Smurf1 ubiquitination by FBXL15 in the context of different E2s, the semi-*in vitro* ubiquitination system was performed with two purified E2s, UbcH5c, and UbcH7, in addition to HA-Ub, E1, purified cell-expressed Flag-FBXL15, and purified bacteria-expressed His-Smurf1. The reaction was incubated at 30°C for 1.5 h and terminated with sample buffer before analysis with anti-Smurf1 antibody. (**D**) SCF$^{GST\text{-}FBXL15}$ complex increases the ubiquitination of Smurf1 *in vitro*. The *in vitro* ubiquitination reactions were performed with the purified HA-Ub, E1, E2 (UbcH5c), purified bacteria-expressed His-Smurf1 (WT or CA), and purified GST-FBXL15 or GST/Cul1/Roc1/Skp1 elution (the Cul1/Roc1/Skp1 were expressed as Myc-tagged proteins in HEK293T cells and the cell lysate was pull down by GSH beads), or GST-FBXL15/Cul1/Roc1/Skp1 complex, as indicated. (**E**) FBXL15 has no effect on Smurf1 auto-ubiquitination. The *in vitro* ubiquitination were performed with the purified HA-Ub, E1/E2, purified bacteria-expressed His-Smurf1 (WT or CA) and purified GST-FBXL15. GST-CKIP-1 was used as a positive control.

for degradation by FBXL15. We observed that in contrast to the significant degradation of Smurf1 WT by FBXL15 (Figure 4A, lanes 1–3), the level of HECT alone was not decreased by FBXL15 (lanes 7–9). In contrast, WW plus HECT was markedly reduced by FBXL15 (lanes 4–6). Examination of the WW plus WW-HECT linker found total three lysines, K324, K355, and K357 (Figure 4A), all of which are located within the WH linker. Deletion of this linker from full-length Smurf1 blocked the FBXL15-promoted Smurf1 degradation (lanes 10–12), indicating that the degradation signal is located within this linker.

Mutations of all three lysines to arginines completely blocked the degradation of Smurf1 by FBXL15 (Figure 4B). Further individual mutation of each lysine showed that K357 was the primary and K355 the secondary site for degradation (Figure 4C). K355 + 357R double mutation resulted in resis-

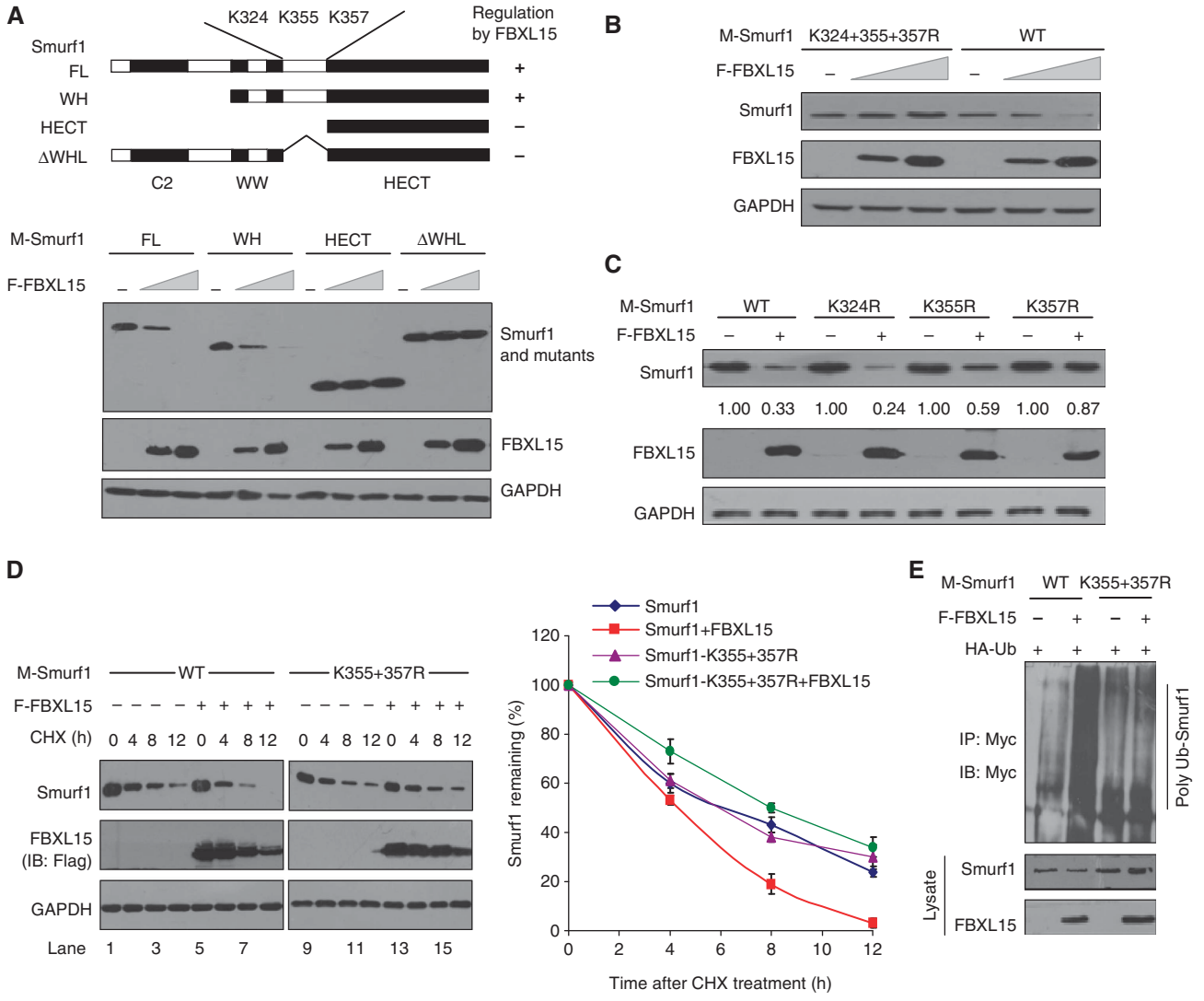

Figure 4 FBXL15 promotes Smurf1 degradation by targeting the sites of Smurf1 K355 and K357. (**A**) A series of Smurf1 deletion mutants were generated (represented in the upper panel) and coexpressed with increasing amounts of FBXL15. Protein levels of Smurf1 wild type and deletions were detected (lower). (**B**) Smurf1 3KR mutation in the WH linker appears to resist degradation by FBXL15. Smurf1 wild type and the indicated mutant were coexpressed with increasing amounts of FBXL15. The Smurf1 protein levels were determined. (**C**) The indicated Smurf1 individual mutants in the WH linker were coexpressed with or without FBXL15. The Smurf1 protein levels were determined and quantified by densitometric analysis. (**D**) HEK293T cells transfected with the indicated plasmids were treated with CHX for the indicated time and then harvested and analysed by western blot. Quantification was performed and each point represents the mean ± s.d. for triplicate experiments. (**E**) Smurf1 2KR mutation attenuates FBXL15-mediated ubiquitination of Smurf1. The ubiquitination assays were performed.

tance against the degradation (Figure 4D, lanes 13–16 versus 5–8) and abrogated the FBXL15-mediated ubiquitination of Smurf1 (Figure 4E). Note that the steady-state level of K355 + 357R in the absence of ectopic FBXL15 gradually decreased upon cycloheximide treatment, as did that of wild-type Smurf1 (Figure 4D, lanes 9–12 versus 1–4), indicating that Smurf1 was also degraded by ligases other than FBXL15, such as the auto-degradation by itself. These data strongly suggest that Smurf1 K357 is the primary ubiquitination site for FBXL15-induced Smurf1 degradation, and K355 is a secondary site.

FBXL15 antagonizes the effect of Smurf1 on BMP signalling

We then sought to better characterize the functional relevance of FBXL15 and Smurf1 for BMP signalling. Ectopic expression of Smurf1 resulted in a dramatic decrease in Smad1 and Smad5, but not Smad3 levels (Figure 5A). Further coexpression of FBXL15 antagonized this effect of Smurf1 (Figure 5A). Upon BMP stimulation, Smurf1 significantly targeted the phosphorylated Smad1/5 for ubiquitination and degradation (Sapkota *et al*, 2007). Through this manner, Smurf1 activation contributes to shut off the BMP signalling. Depletion of FBXL15 resulted in an increased Smurf1 level and attenuated Smad1/5 phosphorylation, even at the early response stage (Figure 5B).

We further delineated the function of FBXL15 in BMP signalling with a luciferase reporter assay. BMP-2 treatment remarkably stimulated the BMP-responsive BRE-luc activity and Smurf1 overexpression inhibited it. When Smurf1 was coexpressed with FBXL15, FBXL15 substantially antagonized the inhibitory effect of Smurf1 (Figure 5C, column 5 versus column 4). In contrast, neither FBXL15 ΔF nor the F-box alone had any significant effect on Smurf1 (columns 6 and 7).

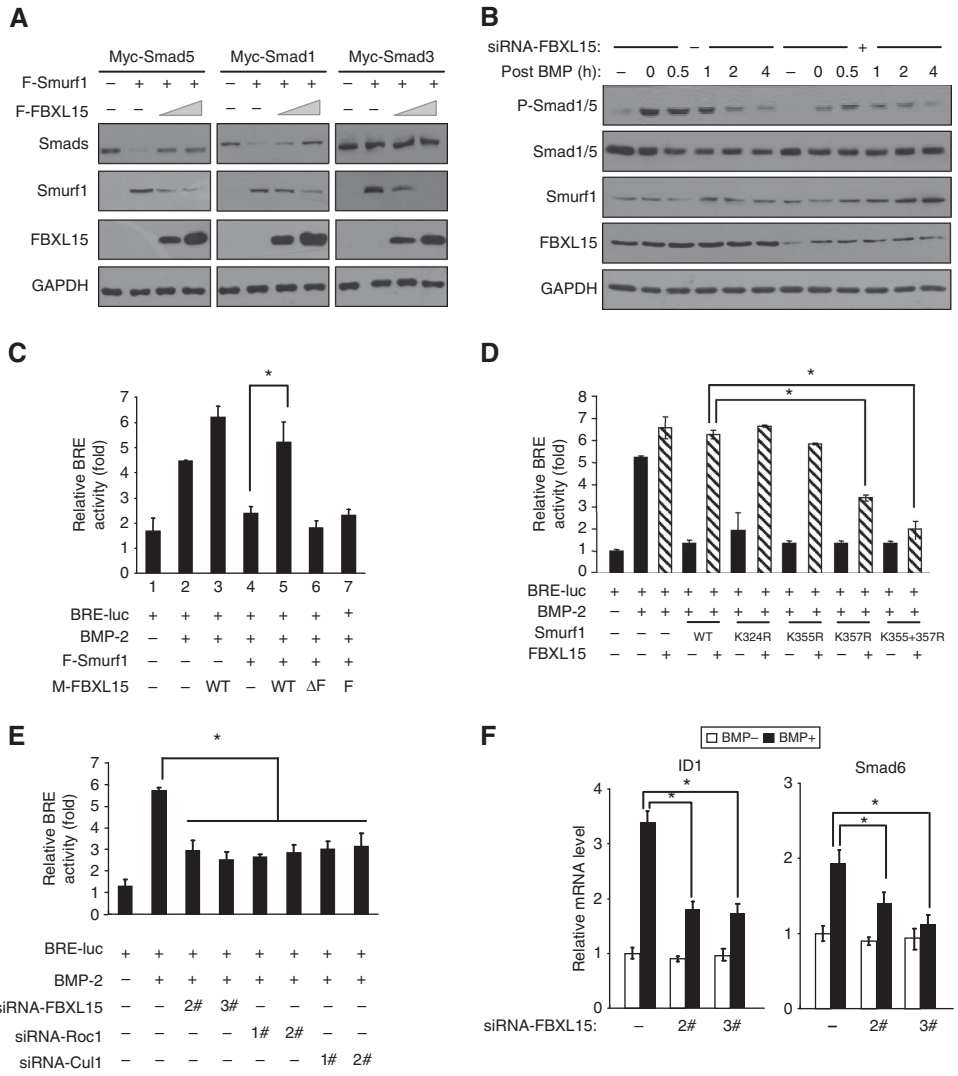

Figure 5 FBXL15 attenuates the effect of Smurf1 on BMP signalling. (**A**) Myc-Smads 1, 3, 5, and constant amounts of Flag-Smurf1 with increasing amounts of Flag-FBXL15 were transfected into HEK293T cells, followed by immunoblotting analysis. (**B**) HepG2 cells were stimulated with BMP-2 (50 ng/ml) for 1 h in the absence or presence of FBXL15 siRNA. Cells were harvested at the indicated times after BMP removal, and total cell lysates were analysed. (**C**) HEK293T cells were transfected with the FBXL15 WT or deletion mutants together with Smurf1, as indicated. Thirty-six hours after transfection, cells were treated with BMP-2 (100 ng/ml) for 12 h before BRE luciferase activity was measured. Data are mean ± s.d. ($n = 3$). (**D**) Effects of FBXL15 on BMP signalling activity by Smurf1 mutants. Reporter activities of BRE-luc in HEK293T cells transfected with a series of Smurf1 mutants, Flag-FBXL15, as indicated, were measured after treatment with BMP-2. Data are mean ± s.d. ($n = 3$). (**E**) Knockdown of endogenous Cullin1, Roc1, or FBXL15 inhibits BMP signalling activity. BMP signalling activity in HepG2 cells was measured by BRE luciferase reporter gene assay. Data are mean ± s.d. ($n = 3$). (**F**) Cells were transfected with siRNA against FBXL15 or non-targeting control siRNA and, 48 h later, treated with BMP-2 (100 ng/ml) or left untreated for 2 h. Expression of BMP target genes ID1, Smad6 was analysed by qRT–PCR. Asterisk means $P < 0.05$.

Additionally, other F-box proteins we examined, including FBXL1/Skp2, FBXL3, FBXL5, and FBXL21, showed no evident antagonistic effects on Smurf1 (Supplementary Figure S4).

To explore whether FBXL15 regulates BMP response through targeting Smurf1, Smurf1 WT and its ubiquitination-resistant mutants were tested for their ability to regulate BRE activity in the absence or presence of ectopic FBXL15 (Figure 5D). As shown, all of the examined Smurf1 forms displayed strong inhibitory effects on BRE activity in the absence of ectopic FBXL15. Coexpression of FBXL15 completely removed the inhibitory effects of Smurf1 WT, K324R and K355R, and partially the K357R mutant. However, FBXL15 failed to reverse that of ubiquitination-resistant K355 + 357R mutant, strongly indicating that FBXL15 regulates the activity of Smurf1 by targeting Smurf1 for ubiquitination and degradation.

Furthermore, we showed that knockdown of endogenous FBXL15 or Cullin1 or Roc1 resulted in reduced stimulation of BRE activity upon BMP-2 treatment (Figure 5E). Depletion of FBXL15 also reduced the upregulation of target genes downstream of Smad1/5 (Figure 5F). Collectively, these data suggest that FBXL15 is a positive regulator of BMP signalling in cultured mammalian cells, at least partially through directing the degradation of Smurf1.

Smurf2 is also ubiquitinated and degraded by FBXL15

Due to the conserved protein sequences and the common domain architecture, we next investigated whether other members of the Nedd4 family could also be regulated by FBXL15. We first examined the association of Nedd4 family members with FBXL15. All nine members, when

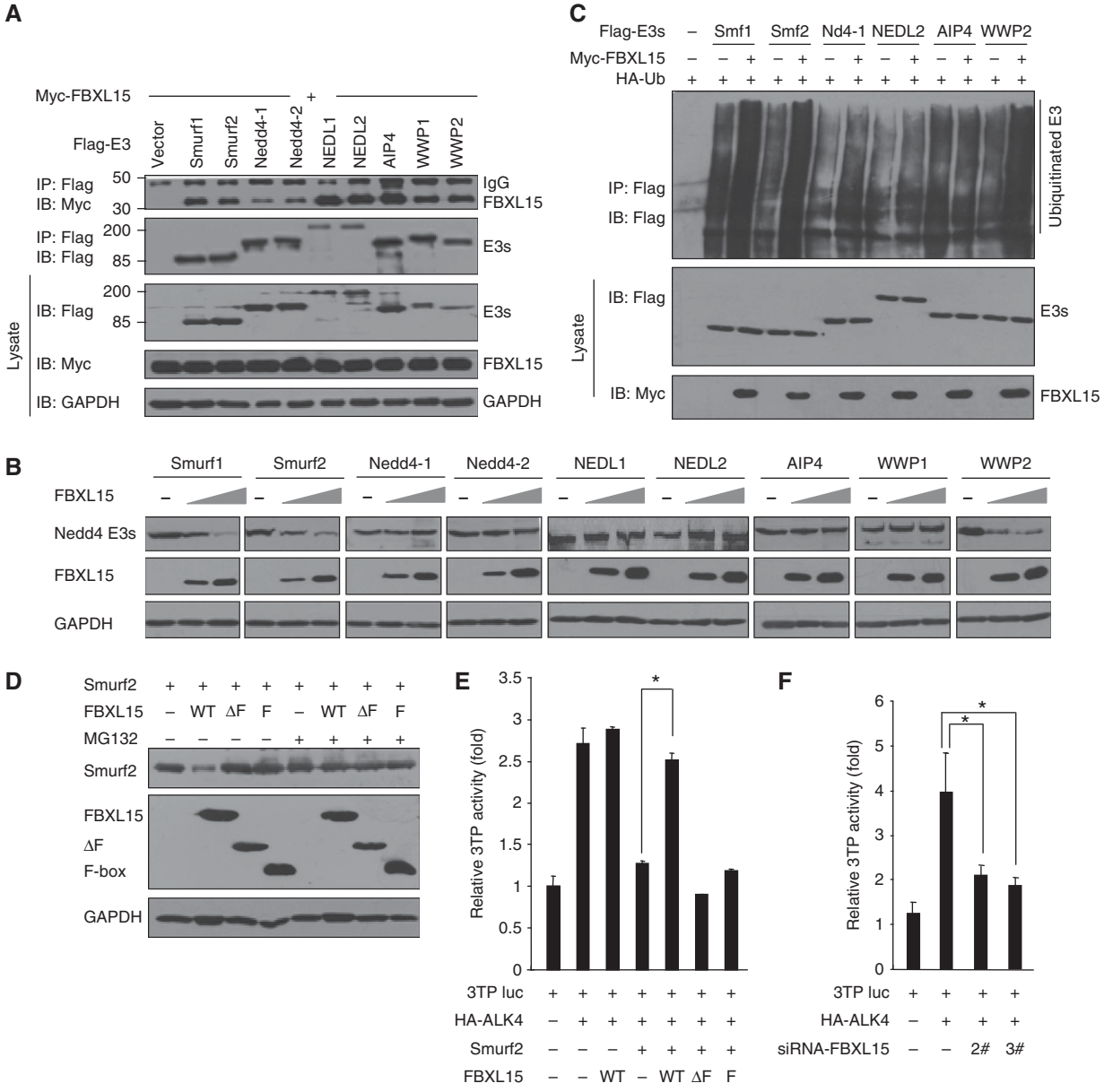

Figure 6 Smurf2 is also targeted for ubiquitination and degradation by FBXL15. (**A**) Interaction analysis of Nedd4 family E3s with FBXL15 by Co-IP assays in HEK293T cells. (**B**) Nedd4 family members were individually cotransfected together with increasing amounts of FBXL15 into HEK293T cells. Their expression levels were determined. (**C**) Ubiquitination levels of Nedd4 family members by FBXL15 were determined through *in vivo* ubiquitination assays. (**D**) FBXL15 WT, but not the indicated mutants, promotes Smurf2 degradation in a proteasome-dependent manner. (**E**) HEK293T cells were transfected with Flag-FBXL15, Flag-FBXL15-ΔF, or Flag-FBXL15-F-box together with Smurf2 and HA-ALK4 before 3TP luciferase activity was measured. Data are mean ± s.d. ($n = 3$). (**F**) Knockdown of endogenous FBXL15 inhibits ALK4-induced 3TP-luc activity. Data are mean ± s.d. ($n = 3$). Asterisk means $P < 0.05$.

expressed in ectopic forms, could be co-immunoprecipitated with FBXL15, although they displayed differential binding affinities (Figure 6A). This result is not surprising, as the HECT large subdomains of each E3 of Nedd4 family exhibit relatively high homologies. Next, we examined whether FBXL15 could control the steady-state levels of these ligases. We observed that Smurf1, Smurf2, and WWP2, but not the other six ligases, were targeted for degradation by FBXL15 (Figure 6B). *In vivo* ubiquitination assays showed that the ubiquitination of Smurf1, Smurf2, and WWP2 could also be significantly enhanced by FBXL15, whereas other E3s could be not (Figure 6C). Among the family, only Smurf2 possesses a lysine identical to the critical ubiquitination site K357 of Smurf1 (Supplementary Figure S5A). WWP2 contains K498 and H500 in the Smurf1 K355- and K357-corresponding positions. Neither K498R nor H500K mutations had any significant effects on the WWP2 ubiquitination promoted by FBXL15 (Supplementary Figure S5B), suggesting that those residues other than K498 and H500 might be responsible for this ubiquitination, which needs further investigations.

The regulatory effects of FBXL15 on Smurf2 stability were further verified. GST pull down and endogenous co-immunoprecipitation assays (Supplementary Figure S6A and B) indicated that Smurf2 could interact with FBXL15 both *in vitro* and endogenously in cultured cells, similar to Smurf1. The degradation–promoting effect of FBXL15

on Smurf2 was dependent on the proteasome activity and the integrity of the SCF complex formed by FBXL15 (Figure 6D). Furthermore, the possible effect of FBXL15 on Smurf2's regulation of TGF-β signalling was measured. Smurf2 overexpression inhibited ALK4-induced activation of TGF-β signalling, and this inhibition was significantly reversed by FBXL15, depending on both the F-box and the LRR domains (Figure 6E). Knockdown of endogenous FBXL15 resulted in a significant decrease in ALK4-induced 3TP-luc activity (Figure 6F). Taken together, these results demonstrate that Smurf2, like Smurf1, is ubiquitinated, degraded, and inhibited by SCF^{FBXL15}.

Zebrafish fbxl15 is required for dorsoventral patterning in early development of embryos

Smurf1 has been demonstrated to antagonize BMP signalling and have a critical role in dorsoventral patterning of *Xenopus* embryos (Zhu *et al*, 1999; Murakami *et al*, 2003; Xia *et al*, 2010). We hypothesized that FBXL15 is involved in embryonic dorsoventral patterning as well. To test this, we used zebrafish as an animal model. We identified a zebrafish cDNA, zgc:85882 (NM_212942), from the GenBank database, which encodes a putative peptide sharing an identity of 65.0% to human FBXL15 (Supplementary Figure S1A) and should be zebrafish *fbxl15*. We first examined the spatiotemporal expression pattern of *fbxl15* during embryonic development by whole-mount *in situ* hybridization. Compared with the sense control (Figure 7A′–E′), *fbxl15* is maternally expressed and its transcriptions are evenly distributed until the 6-somite stage (Figure 7A–D). At 24 h postfertilization (hpf), *fbxl15* transcripts are mainly present in head region (Figure 7E). The existence of *fbxl15* transcripts in early embryos suggests a potential function in early development.

Next, we investigated *fbxl15* function in the zebrafish embryos by knocking down *fbxl15* expression with two different morpholinos of *fbxl15*. Both morpholinos efficiently blocked the expression of fbxl15-5′UTR-GFP fusion plasmid in zebrafish embryos, while the control morpholino fbxl15-cMO1 with mismatched nucleotides for fbxl15-MO1 had no effect (Supplementary Figure S7). Injection of 7.5 ng fbxl15-MO1 into one- to two-cell wild-type embryos resulted in a kind of classic dorsalized phenotype at 24 hpf, manifesting a shorter and curved posterior trunk, together with extensive cell death in the neural system (Figure 7F–H). Since morpholinos often cause certain degrees of apoptosis due to off-target activation of *p53* (Robu *et al*, 2007), we co-injected 7.5 ng fbxl15-MO1 and 7.5 ng p53-MO to block the non-specific effect. Such a co-injection still led to the dorsalized phenotype, but avoided widespread cell death (Figure 7I), which suggests a *bona fide* requirement of *fbxl15* for early development.

To further confirm the implication of *fbxl15* in dorsoventral patterning, we examined the expression of some dorsal and ventral markers at the shield stage. In fbxl15-MO1-injected embryos, the expression of the dorsal marker *gsc* was expanded (100%, $n=92$), while the expression of the ventral markers *eve1* (87.5%, $n=96$) and *gata2* (100%, $n=87$) were almost eliminated. Compared with fbxl15-MO1 injection alone, co-injection of 50 pg *fbxl15* mRNA had a partial rescue on the marker genes expression. For example, only 60.3% of embryos showed *gsc* expansion ($n=58$), 40.9 and 44.9% showed *eve1* ($n=66$) and *gata2* ($n=107$) reduction (Figure 7J–M). Similar phenotype was observed with fbxl15-MO2 (Supplementary Figure S8). In addition, the rescue effect was confirmed by qRT–PCR experiments as shown in Figure 7N. Taken together, these results suggest that *fbxl15* is required for the specification of the dorsoventral fate during embryonic development.

Fbxl15 contains an N-terminal F-box domain, which mediates binding to Skp1 and then is linked to the rest of the SCF complex. Injection of 100 pg *fbxl15-ΔF* mRNA caused *gsc* expansion and *eve1* and *gata2* reduction (Supplementary Figure S8), which mimicked the effect of fbxl15-MOs. These results suggested that Fbxl15-ΔF functions as a dominant-negative form and F-box domain is essential for the roles of FBXL15 in dorsoventral patterning in zebrafish embryos. Additionally, overexpression of 50 pg *skp1* mRNA or 50 pg *fbxl15* mRNA, respectively, almost had no effect on *gsc* expression at shield stage, while co-injection of these two mRNA was able to cause obvious inhibition of *gsc* at the same stage (Supplementary Figure S9). It is indicated that Fbxl15 can work together with Skp1 to regulate the dorsoventral patterning in zebrafish embryos. In the light of the results mentioned above, we speculate that Fbxl15 functions dependently on the SCF complex.

Furthermore, we tested the ability of Fbxl15 to degrade Smurf1 in zebrafish embryos. Compared with *gfp* mRNA injection (Supplementary Figure S10A), injection of *smurf1-gfp* fusion mRNA produced weaker GFP fluorescence (Figure 7O). Co-injection of *fbxl15* mRNA with *gfp* mRNA did not change GFP fluorescence levels (Supplementary Figure S10B), but *fbxl15* and *smurf1-gfp* mRNA co-injection produced extremely low levels of GFP fluorescence (Figure 7P). Correspondingly, co-injection of fbxl15-MO1 or fbxl15-MO2, respectively, both enhanced the Smurf1-GFP fluorescence in zebrafish embryos at the same stage (Figure 7Q and R). These results imply that Fbxl15 is able to destabilize Smurf1-GFP. As demonstrated above, FBXL15-promoted Smurf1 degradation *in vitro* requires K355 and K357 within the WW-HECT linker region. We found that fluorescence produced in zebrafish embryos by Smurf1Mt-GFP that had K355R and K357R mutations in Smurf1 was not affected by *fbxl15* mRNA injection (Figure 7S and T). Similarly, *fbxl15* overexpression promoted degradation of Smurf2-GFP in zebrafish embryos (Figure 7U and V). We conclude that Fbxl15 has the ability to facilitate Smurf1 and Smurf2 degradation in zebrafish embryos.

FBXL15 is involved in the regulation of bone homoeostasis in adult rats

We next asked whether FBXL15 also has a role in adult development, especially in the maintenance of bone homoeostasis. Smurf1 has been determined to specifically suppress bone formation in mammals (Zhao *et al*, 2003, 2010; Yamashita *et al*, 2005). Consistent with this notion, the deficiency of its auxiliary factor CKIP-1 in mice resulted in augmented bone mass and enhanced osteoblast activity as well as reduced Smurf1 activity (Lu *et al*, 2008). We then hypothesized that FBXL15, as a negative regulator of Smurf1, has a positive role in bone formation. If true, FBXL15 depletion should lead to a decrease in bone mass.

To verify this hypothesis, we evaluated the effect of FBXL15 depletion by RNA interference (RNAi) in normal adult rats on bone mass. First, we designed three independent siRNAs

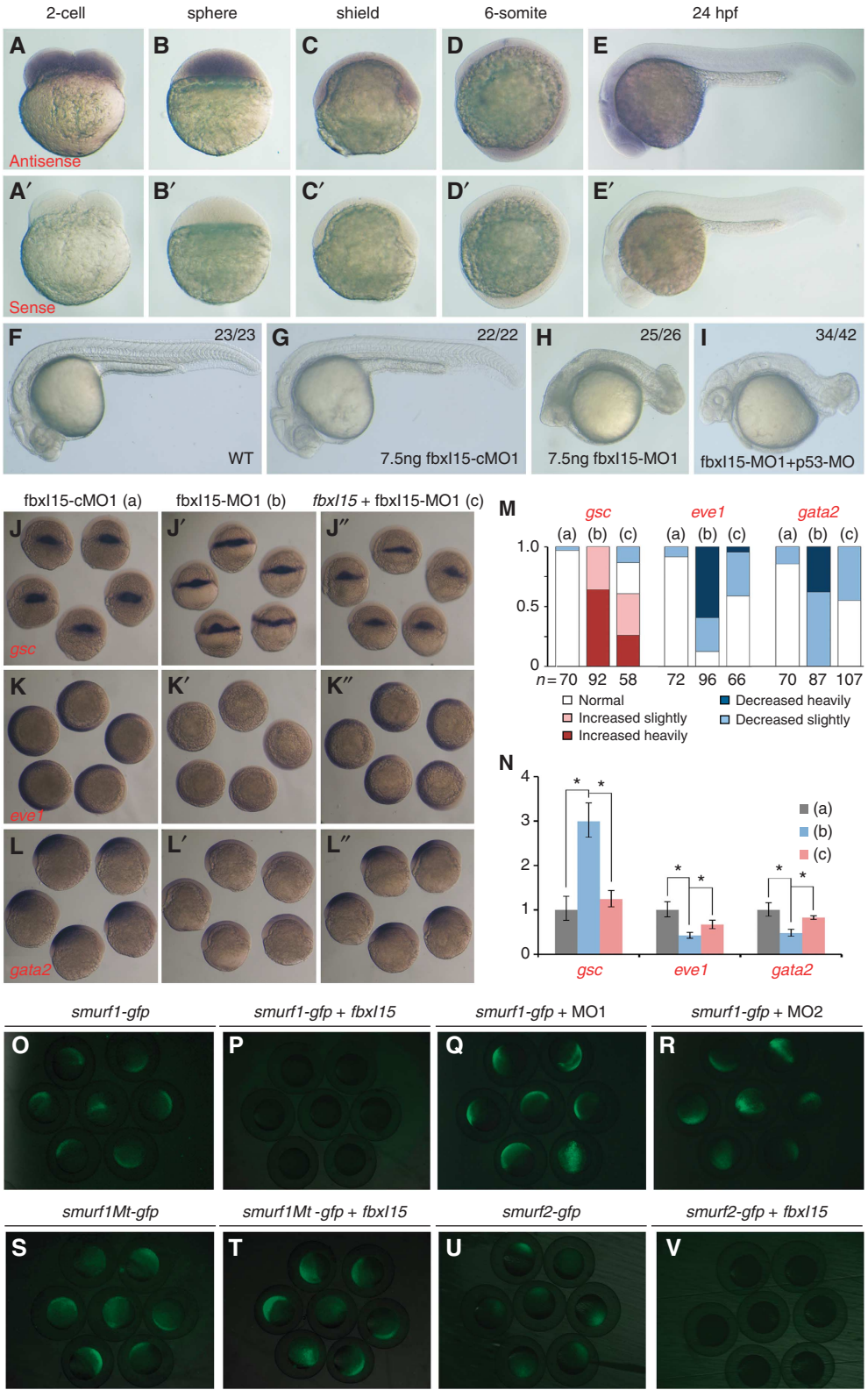

Figure 7 *fbxl15* is expressed in zebrafish embryos and required for dorsoventral development. (**A**–**E**) The expression pattern of *fbxl15* in zebrafish embryos at indicated stages, detected by whole-mount *in situ* hybridization. Lateral views: (**A′**–**E′**) indicate sense probe. (**F**–**I**) Knockdown of *fbxl15* caused dorsalized phenotypes. Wild-type embryos were injected with morpholinos at one- to two-cell stages and observed at 24 hpf. Quantification result is also shown. (**J**–**N**) Knockdown of *fbxl15* altered dorsal (*gsc*) and ventral (*eve1* and *gata2*) markers expression at the shield stage. Injection doses: fbxl15-MO1 (**J′**–**L′**) or fbxl15-cMO1 (**J**–**L**), 7.5 ng; *fbxl15* mRNA (**J″**–**L″**), 50 pg. Dorsal views with animal pole to the top for *gsc*; animal views with dorsal to the right for *eve1*; lateral views with dorsal to the right for *gata2*. Statistical data and qRT–PCR results for maker changes in (**J**–**L″**) are shown in (**M**) and (**N**). Asterisk means $P<0.05$. (**O**–**V**) Overexpression or knockdown of *fbxl15* affects the stability of Smurf-GFP proteins. The *smurf1Mt* is a mutant form with K355R and K357R for *smurf1*. Wild-type embryos were injected at one- to two-cell stages with indicated synthetic mRNAs or MOs and observed at mid-gastrulation stages. Injection doses: 200 pg for *smurf1-gfp*, *smurf1Mt-gfp* or *smurf2-gfp* mRNA; 300 pg for *fbxl15* mRNA; 7.5 ng for fbxl15-MO1; and 12.5 ng for fbxl15-MO2.

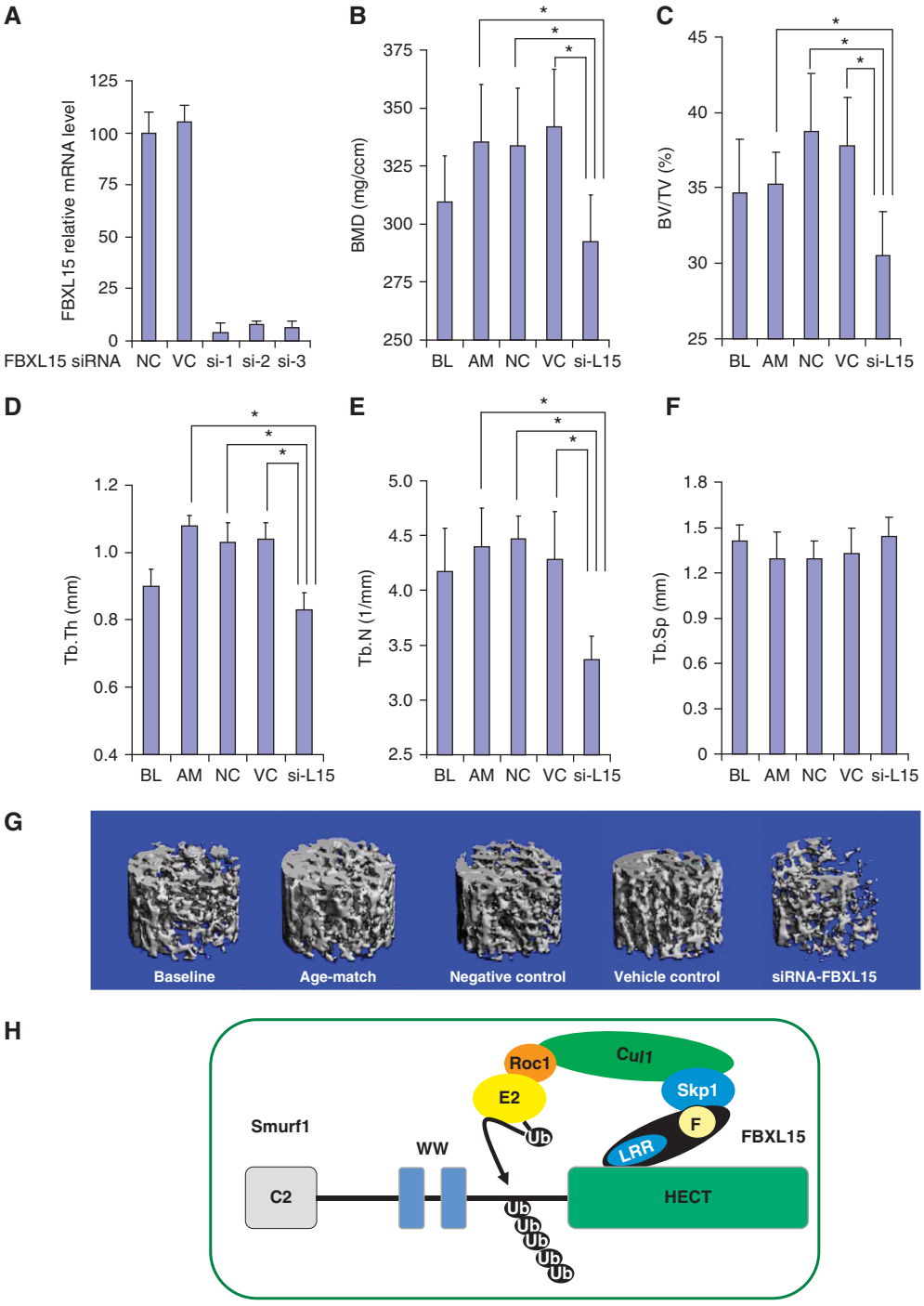

Figure 8 FBXL15 regulates bone homoeostasis in adult rats. (**A**) The rat osteoblast-like UMR106 cells were transfected with non-targeting siRNA (NC), vehicle control (VC), and three independent siRNAs against rat FBXL15. The efficiency of FBXL15 knockdown was determined by qRT–PCR to analyse the mRNA levels of FBXL15. (**B**–**F**) MicroCT analysis of trabecular bone at proximal tibia in five groups of rats. Thirty 6-month-old female Sprague–Dawley rats were divided into the siRNA (#1) treatment group (FBXL15 RNAi group), the non-targeting siRNA control group (NC group), the vehicle control group (VC group), the age-matched group (AM group) and the baseline group (BL group) as described in the Materials and methods. The following parameters bone mineral density (BMD), relative bone volume (BV/TV), trabecular number (Tb.N), trabecular thickness (Tb.Th), and trabecular separation (Tb.Sp) were analysed, and data are presented as mean ± s.d. Asterisk means $P<0.05$. (**G**) Representative three-dimensional reconstruction images of trabecular bone at the proximal tibia from the baseline group (Bl group), AM group, non-targeting siRNA control group (NC group), vehicle control group (VC group), and FBXL15 siRNA treatment group (RNAi group). (**H**) Schematic representation of Smurf1 regulation by SCF^{FBXL15} complex.

specifically targeting the rat FBXL15 gene and determined the knockdown efficiency in the rat osteoblast-like cell line UMR106. Quantitative real-time PCR analysis showed that all of the examined three siRNAs displayed high knockdown efficiency of >90% (Figure 8A). Second, the siRNA #1 with the highest knockdown efficiency (96.4%) were integrated with a liposome-based bone-targeting delivery system (BTDS) (Jeffs *et al*, 2005) to be delivered to and enriched at the bone formation surface. Third, we examined the apparent bone mineral density (apparent BMD), three-dimensional ar-

chitecture parameters, and bone histomorphometric parameters in trabecular bone after administration of the FBXL15 siRNA in 6-month-old female rats. The microCT analysis showed that FBXL15 siRNA treatment for 6 weeks significantly decreased the apparent BMD, relative bone volume, trabecular thickness (Tb.Th), and trabecular number (Tb.N) compared with the age-matched (AM) group, non-sense siRNA group (NC), or BTDS only group (without siRNA) (VC) ($P<0.05$ for all) (Figure 8B–E). No significant difference was found in trabecular separation among all the groups ($P>0.05$) (Figure 8F). Importantly, less organized three-dimensional architecture and lower bone mass in trabecular bone were clearly found in the rats treated with the FBXL15 siRNA compared with the above control groups (Figure 8G). Overexpression of FBXL15 in rat osteoblast cell line UMR106 was sufficient to induce an increase of ALP activity, but the FBXL15-ΔF was not (Supplementary Figure S11). Collectively, these data strongly indicate that FBXL15 is a positive regulator of bone mass maintenance in adult mammals.

Discussion

Compared with RING-type E3s, there still remain many more unanswered questions regarding HECT-type E3s, among which the question how HECT domain E3 activity is regulated constitutes a particularly significant gap. Nedd4 family members are the best characterized subgroup of HECT-type E3s, and several mechanisms in multiple layers of regulation have been determined, such as E3-substrate recognition, E2–E3-binding affinity, and relief of intra-molecular autoinhibition (Ogunjimi *et al*, 2005; Gallagher *et al*, 2006; Oliver *et al*, 2006; Oberst *et al*, 2007; Wiesner *et al*, 2007; Bruce *et al*, 2008; Lu *et al*, 2008; Mund and Pelham, 2009). Among this family, Smurf1 and Smurf2 are attractive because they have an important role in the regulation of adult bone remodelling, embryonic development and tumourigenesis through controlling the BMP/TGF-β, Wnt-PCP, and RhoA pathways (Zhu *et al*, 1999; Wang *et al*, 2003; Zhao *et al*, 2003; Izzi and Attisano, 2004; Yamashita *et al*, 2005; Chen and Matesic, 2007; Bernassola *et al*, 2008; Inoue and Imamura, 2008; Suzuki *et al*, 2008; Jin *et al*, 2009; Narimatsu *et al*, 2009). Although recent studies have identified the activation mechanisms of Smurf1 (Lu *et al*, 2008) and Smurf2 (Ogunjimi *et al*, 2005; Wiesner *et al*, 2007) by CKIP-1 and Smad7, respectively, how their activity is negatively regulated still remains unclear.

In this study, we identified an F-box protein FBXL15 as a substrate-recognizing subunit of the SCF ligase complex to target Smurf1, and also Smurf2, for ubiquitination and proteasomal degradation (Figure 8H). FBXL15 interacts with Skp1 and Smurf1 through its F-box and LRR domains, respectively; thereby promotes the ubiquitination of Smurf1 on two lysines within the WW-HECT linker. The degradation of Smurf1 by FBXL15 is dependent on the integrity of a functional SCF complex. To our knowledge, this is the first case to show a typical HECT E3 (Smurf1) acts as a substrate to be degraded *in trans* by a RING E3, especially by a multi-subunit SCF complex. Under the *in vitro* ubiquitination assay system, FBXL15 alone seems not to change the auto-ubiquitination ability of Smurf1 itself, whereas the previous identified Smurf1 co-factor, CKIP-1 (Lu *et al*, 2008), can do it (Figure 3E). Also, depletion of Smurf2 in human embryonic kidney HEK293T cells also had no significant effects of the FBXL15 on Smurf1 ubiquitination (Supplementary Figure S3). However, we cannot rule out the possibility that the SCF^{FBXL15} ligase complex coordinates with Smurf1 to control the ubiquitination and stability of Smurf1 itself, since the purified Cullin1/Roc1/Skp1 complex in the ubiquitination assays of this study (Figure 3D) might also co-purify the endogenous FBXL15 and Smurf1 proteins. In addition, we cannot rule out the possibility that SCF^{FBXL15} complex might coordinate with Smurf2 to control Smurf1 stability in certain cell types or pathophysiological conditions. In this regard, a recent study showed that Smurf2 interacts with Smurf1 to induce the degradation of Smurf1 to prevent migration of breast cancer cells (Fukunaga *et al*, 2008). Previous studies have shown that RING E3s can be targeted by certain HECT E3s; for example, Cbl is degraded by Nedd4-1 and Itch/AIP4 (Magnifico *et al*, 2003), whereas RNF11 is a target of Smurf2 (Subramaniam *et al*, 2003). A recent study demonstrated that the N-end rule pathway is mediated by a complex of RING-type Ubr1 and HECT-type Ufd4 ligases (Hwang *et al*, 2010). Our current data, combined with these reports, suggest that the crosstalk between RING E3 and HECT E3 may be more general than once thought.

WW domains of Smurf1 function as the substrate-recognition module, whereas the HECT C-lobe and the small subdomain of the N-lobe are responsible for ubiquitin thioester intermediate formation and E2 binding, respectively (Huang *et al*, 1999; Rotin and Kumar, 2009). The WW domains linker is also involved in the substrate binding and functions as an adaptor-targeting site for Smurf activation (Lu *et al*, 2008; Chong *et al*, 2010). In contrast, the function of HECT N-lobe large subdomain and the role of WW-HECT linker are still unknown. This study provides new insight into these issues: the large subdomain is the recognition site of FBXL15, and the WH linker contains the ubiquitination sites K355 and K357 (Figure 8H). Consistent with the former notion, all nine members of Nedd4 family were co-immunoprecipitated with FBXL15, implying that the HECT large subdomain contains a certain motif or sequence that is commonly recognized by the LRR domain. Therefore, the *in trans* ubiquitination represents a novel regulatory mechanism to coordinate the homoeostasis of Smurf1/2 and the linker regions may serve as regulatory sites for E3 activity.

One of the long-standing central issues in SCF ligase studies is to identify the physiological substrates, as the substrates of nearly two-thirds of F-box proteins have not been characterized (Skaar *et al*, 2009a, b). In this regard, this study identified Smurf1 and Smurf2 as endogenous substrates of FBXL15 (but not other F-box proteins) and highlighted a positive role of FBXL15 in BMP signalling both in zebrafish and in mammals. Depletion of *fbxl15* in zebrafish embryos resulted in embryonic dorsalization with altered dorsal and ventral marker expression (Figure 7), mimicking *bmp2b*-deficient mutant swirl (Kishimoto *et al*, 1997) and *bmp7*-deficient mutant snailhouse (Dick *et al*, 2000). This evidence is the first to directly show a role for an F-box protein in the determination of the dorsalization–ventralization axis. Furthermore, FBXL15 depletion in adult rats resulted in a decrease of bone mass, bone mineral density, Tb.N and Tb.Th (Figure 8). Although we cannot rule out the possibility that FBXL15 may target more substrates than Smurf1/2 in different tissues or developmental stages, our present evidence at least partially reflects the *in vivo*

physiological relevance between FBXL15 and Smurf1. Deeper investigations surely need to be performed to verify the significance of FBXL15 *in vivo* and the correlation between FBXL15 and Smurfs in certain spatial-temporal conditions. Generation of an *FBXL15*-deficient mice model should represent one of such approaches and is now in preparation.

Materials and methods

Immunoprecipitation and immunoblotting

For general cell lysis, transfected cells were harvested and lysed in HEPES lysis buffer (20 mM HEPES pH 7.2, 50 mM NaCl, 0.5% Triton X-100, 1 mM NaF, 1 mM dithiothreitol) for 30 min at 4°C and boiled with 2 × SDS/PAGE loading buffer for 10 min. For immunoprecipitation, cell lyates were prepared in 500 μl HEPES buffer supplemented with protease inhibitor cocktail (Roche) and phosphatise inhibitors (10 mM NaF and 1 mM Na_3VO_4). Immunoprecipitations were performed using mouse anti-Myc (2 μg, MBL), anti-Flag (2.5 μg, Sigma), or Smurf1 (2 μg, Abcam) monoclonal antibodies for 4 h at 4°C followed by incubation with protein A/G-agarose beads (Santa Cruz) overnight at 4°C. Beads were then washed three times in HEPES lysis buffer and examined by immunoblotting with the indicated primary antibodies and appropriate secondary antibody, followed by detection with SuperSignal chemiluminescence kit (Pierce). Quantification of the visualized bands by densitometry was analysed using Scion Image software.

In vivo ubiquitination assays

To determine *in vivo* ubiquitination, HEK293T cells were transiently transfected with HA-ubiquitin, FBXL15, and either Smurf1 (WT/CA/K355 + 357R) or other members of Nedd4 family, as indicated. Thirty-six hours after transfection, cells were treated with MG132 for 12 h and then cells were harvested. To rule out non-specific ubiquitinaton detection, immunoprecipitations were prepared in 500 μl denatured modified RIPA buffer (10 mM Tris–HCl, pH 7.5/5 mM EDTA, 150 mM NaCl, 1% Nonidet P-40, 1% sodium deoxycholate, 0.025% SDS, protease inhibitors) supplemented with protease inhibitor cocktail (Roche) and phosphatase inhibitors (10 mM NaF and 1 mM Na_3VO_4) and then incubated with anti-Myc, anti-Smurf1, or anti-Flag antibody for 3 h and protein A/G-agarose beads for another 8 h at 4°C. After washing for three times, ubiquitinated conjugates were detected by immunoblotting with indicated antibodies.

In vitro ubiquitination assays

His-Smurf1 (wild type and C699A mutant) and GST-FBXL15 were expressed in *Escherichia coli* BL21 and purified according to the manufacturer's instructions. $SCF^{GST\text{-}FBXL15}$ and $SCF^{GST\text{-}FBXL15\text{-}\Delta F}$ complexes were purified by GST-affinity column from HEK293T cell lysates expressing GST-FBXL15 or GST-FBXL15-ΔF, together with Myc-Cul1, Myc-Skp1, and Flag-Roc1. Cul1, Skp1, and Roc1 proteins were purified by immunoprecipitation with Myc-antibody or Flag-antibody plus protein A/G agarose. The assays to assess the *in vitro* ubiquitination of Smurf1 were carried out in 30 μl ubiquitination assay buffer (50 mM Tris pH 8.0, 50 mM NaCl, 1 mM DTT, 5 mM $MgCl_2$, and 3 mM ATP), with 0.7 μg of E1, 1 μg of UbcH5c (E2), 15 μg HA-ubiquitin (all from Boston Biochem), 0.7 μg of His-Smurf1 (wild type or mutant as indicated), and 1.5 μg GST-FBXL15 or $SCF^{GST\text{-}FBXL15}$ or $SCF^{GST\text{-}FBXL15\text{-}\Delta F}$ complexes (SCF complex contains Myc-Cul1, Myc-Skp1, Flag-Roc1, and GST-FBXL15 or GST-FBXL15-ΔF) were incubated at 30°C for 1.5 h and terminated with sample buffer before western blotting with anti-Smurf1 monoclonal antibody.

RNA interference

The FBXL15 siRNA-targeting human FBXL15 (1#: 5′-CACCCUGGAGCUUCAAAUATT-3′, 2#: 5′-GGAACUGCCCAGAACUCCATT-3′, 3#: 5′-GCCUGAGCCGCUUGCGGAATT-3′), the FBXL15 siRNA-targeting rat FBXL15 (1#: 5′-CACCCUUUGUCAACCUACATT-3′, 2#: 5′-CACCCUGGAAUUUCAAAUATT-3′, 3#: 5′-GGCCAAAGCUAGUAAAGCUTT-3′), the Cullin1 siRNA (1#: 5′-GGUUAUAUCAGUUGUCUAA-3′, 2#: 5′-CAACGAAGAGUUCAGGUUU-3′), the Roc1 siRNA (1#: 5′-GAAGCGCUUUGAAGUGAAA-3′, 2#: 5′-GCAUAGAAUGUCAAGCUAA-3′) (Salahudeen *et al*, 2009), the Smurf2 siRNA (5′-CCUUCUGUGUUGAACAUAA-3′), and the non-targeting siRNA (5′-UUCUCCGAACGUGUCACGUTT-3′) were synthesized by Shanghai GenePharm. All siRNA transfections were performed using Lipofectamine 2000 (Invitrogen) according to the commercialized protocol, and the RNAi efficiency was assessed by western blot analysis.

Fish embryos

Zebrafish Tuebigen strain was used. Embryos were raised in Holtfreter's solution at 28.5°C and staged as previously described (Kimmel *et al*, 1995).

mRNAs, morpholinos, and microinjection in zebrafish embryos

mRNA was *in vitro* synthesized using mMESSAGE mMACHINE® kit (Ambion), purified with RNeasy Mini kit (Qiagen), and dissolved in RNase-free water. Morpholinos were synthesized by Gene Tools, LLC, and dissolved in water. The related morpholinos sequences were as follows: fbxl15-MO1, 5′-CAGGTTTTTGATCCATGCTGACACT-3′, blocking translation of *fbxl15*; fbxl15-cMO1, 5′-CAGCTTT TTCATCGATGGTCACAGT-3′, a control morpholino with six mismatched nucleotides (underlined) according to fbxl15-MO1; fbxl15-MO2, 5′- CCTGTGGTCCGTGTACATTATTATT-3′, blocking translation of *fbxl15*; p53-MO, 5′-GACCTCCTCTCCACTAAACTA CGAT-3′, which was used to suppress non-specific activation of morpholinos (Robu *et al*, 2007). The 5′UTR of Zebrafish *fbxl15* was amplified by PCR and inserted into *Xho*I and *Bam*HI sites of pEGFP-N3 vector for examining the efficiency of fbxl15-MO. About 1–1.5 nl mRNAs or morpholinos solution was injected into embryos at one- to two-cell stages. When co-injection of mRNA and morpholino was performed, the mRNA was first injected, followed by the morpholino injection. For mRNA rescue experiment, the *fbxl15* sequence region complementary to the fbxl15-MO1 sequence was mutated by PCR with the modified forward primer 5′-GGAATTCCACCATGGACCAGAAGCCGGACGAGCGCATGCAAAGCC-3′, so that fbxl15-MO1 could not bind to the modified *fbxl15* mRNA. The mutant *fbxl15*-Δ*F* is constructed by deleted F-box domain (1–66 amino acids) at the NH_2 terminus of *fbxl15*.

Whole-mount in situ hybridization

Digoxigenin-UTP-labelled antisense RNA probes were generated by *in vitro* transcription with Roche kit. Whole-mount *in situ* hybridization followed the standard procedure. The stained embryos after *in situ* hybridization and GFP-expressing embryos were photographed using an SPOT Insight camera under the Leica MZ16 microscope.

Statistical analysis

Statistical evaluation was carried out using a Student's *t*-test.

Supplementary data

Supplementary data are available at *The EMBO Journal* Online (http://www.embojournal.org).

Acknowledgements

We thank Drs Dahua Chen, Di Chen, Ye-Guang Chen, Hugues Dardente, Kohei Miyazono, Yongfeng Shang, Wesley I Sundquist, James A Wohlschlegel and Yue Xiong for providing materials. This research was supported by the Chinese National Basic Research Programs (2011CB910602, 2007CB914601), the Chinese National Natural Science Foundation Projects (31071233, 30830029, 30970601, 30830068, 30921004) and the National Key Technologies R&D Program for New Drugs (2009ZX09503-002, 2009ZX09301-002).

Author contributions: LZ, FH, and SJ co-organized and performed project planning, data analysis, discussion, and writing; YC and SH performed the main experimental work of Smurf1-FBXL15 interaction, Smurf1 ubiquitination by FBXL15, and molecular mechanism investigations; CX performed the main experimental work of FBXL15 function analysis in zebrafish embryos; KL and GX participated in the bone homoeostasis analysis; JW performed the yeast two-hybrid screening; AM was involved in the zebrafish phenotype analysis.

Conflict of interest

The authors declare that they have no conflict of interest.

References

Bernassola F, Karin M, Ciechanover A, Melino G (2008) The HECT family of E3 ubiquitin ligases: multiple players in cancer development. *Cancer Cell* **14:** 10–21

Bruce MC, Kanelis V, Fouladkou F, Debonneville A, Staub O, Rotin D (2008) Regulation of Nedd4-2 self-ubiquitination and stability by a PY motif located within its HECT-domain. *Biochem J* **415:** 155–163

Cardozo T, Pagano M (2004) The SCF ubiquitin ligase: insights into a molecular machine. *Nat Rev Mol Cell Biol* **5:** 739–751

Chen C, Matesic LE (2007) The Nedd4-like family of E3 ubiquitin ligases and cancer. *Cancer Metastasis Rev* **26:** 587–604

Chong PA, Lin H, Wrana JL, Forman-Kay JD (2010) Coupling of tandem Smad ubiquitination regulatory factor (Smurf) WW domains modulates target specificity. *Proc Natl Acad Sci USA* **107:** 18404–18409

Dick A, Hild M, Bauer H, Imai Y, Maifeld H, Schier AF, Talbot WS, Bouwmeester T, Hammerschmidt M (2000) Essential role of Bmp7 (snailhouse) and its prodomain in dorsoventral patterning of the zebrafish embryo. *Development* **127:** 343–354

Fukunaga E, Inoue Y, Komiya S, Horiguchi K, Goto K, Saitoh M, Miyazawa K, Koinuma D, Hanyu A, Imamura T (2008) Smurf2 induces ubiquitin-dependent degradation of Smurf1 to prevent migration of breast cancer cells. *J Biol Chem* **283:** 35660–35667

Gallagher E, Gao M, Liu YC, Karin M (2006) Activation of the E3 ubiquitin ligase Itch through a phosphorylation-induced conformational change. *Proc Natl Acad Sci USA* **103:** 1717–1722

Hershko A, Ciechanover A (1998) The ubiquitin system. *Annu Rev Biochem* **67:** 425–479

Huang L, Kinnucan E, Wang G, Beaudenon S, Howley PM, Huibregtse JM, Pavletich NP (1999) Structure of an E6AP-UbcH7 complex: insights into ubiquitination by the E2-E3 enzyme cascade. *Science* **286:** 1321–1326

Hwang CS, Shemorry A, Auerbach D, Varshavsky A (2010) The N-end rule pathway is mediated by a complex of the RING-type Ubr1 and HECT-type Ufd4 ubiquitin ligases. *Nat Cell Biol* **12:** 1177–1185

Inoue Y, Imamura T (2008) Regulation of TGF-beta family signaling by E3 ubiquitin ligases. *Cancer Sci* **99:** 2107–2112

Izzi L, Attisano L (2004) Regulation of the TGFbeta signalling pathway by ubiquitin-mediated degradation. *Oncogene* **23:** 2071–2078

Jeffs LB, Palmer LR, Ambegia EG, Giesbrecht C, Ewanick S, MacLachlan I (2005) A scalable, extrusion-free method for efficient liposomal encapsulation of plasmid DNA. *Pharmaceutical Res* **22** (3)**:** 362–372

Jin C, Yang YA, Anver MR, Morris N, Wang X, Zhang YE (2009) Smad ubiquitination regulatory factor 2 promotes metastasis of breast cancer cells by enhancing migration and invasiveness. *Cancer Res* **69:** 735–740

Jin J, Cardozo T, Lovering RC, Elledge SJ, Pagano M, Harper JW (2004) Systematic analysis and nomenclature of mammalian F-box proteins. *Genes Dev* **18:** 2573–2580

Kimmel CB, Ballard WW, Kimmel SR, Ullmann B, Schilling TF (1995) Stages of embryonic development of the zebrafish. *Dev Dyn* **203:** 253–310

Kishimoto Y, Lee KH, Zon L, Hammerschmidt M, Schulte-Merker S (1997) The molecular nature of zebrafish swirl: BMP2 function is essential during early dorsoventral patterning. *Development* **124:** 4457–4466

Li S, Lu K, Wang J, An L, Yang G, Chen H, Cui Y, Yin X, Xie P, Xing G, He F, Zhang L (2010) Ubiquitin ligase Smurf1 targets TRAF family proteins for ubiquitination and degradation. *Mol Cell Biochem* **338:** 11–17

Lu K, Yin X, Weng T, Xi S, Li L, Xing G, Cheng X, Yang X, Zhang L, He F (2008) Targeting WW domains linker of HECT-type ubiquitin ligase Smurf1 for activation by CKIP-1. *Nat Cell Biol* **10:** 994–1002

Magnifico A, Ettenberg S, Yang C, Mariano J, Tiwari S, Fang S, Lipkowitz S, Weissman AM (2003) WW domain HECT E3s target Cbl RING finger E3s for proteasomal degradation. *J Biol Chem* **278:** 43169–43177

Mund T, Pelham HR (2009) Control of the activity of WW-HECT domain E3 ubiquitin ligases by NDFIP proteins. *EMBO Rep* **10:** 501–507

Murakami G, Watabe T, Takaoka K, Miyazono K, Imamura T (2003) Cooperative inhibition of bone morphogenetic protein signaling by Smurf1 and inhibitory Smads. *Mol Biol Cell* **14:** 2809–2817

Narimatsu M, Bose R, Pye M, Zhang L, Miller B, Ching P, Sakuma R, Luga V, Roncari L, Attisano L, Wrana JL (2009) Regulation of planar cell polarity by Smurf ubiquitin ligases. *Cell* **137:** 295–307

Oberst A, Malatesta M, Aqeilan RI, Rossi M, Salomoni P, Murillas R, Sharma P, Kuehn MR, Oren M, Croce CM, Bernassola F, Melino G (2007) The Nedd4-binding partner 1 (N4BP1) protein is an inhibitor of the E3 ligase Itch. *Proc Natl Acad Sci USA* **104:** 11280–11285

Ogunjimi AA, Briant DJ, Pece-Barbara N, Le Roy C, Di Guglielmo GM, Kavsak P, Rasmussen RK, Seet BT, Sicheri F, Wrana JL (2005) Regulation of Smurf2 ubiquitin ligase activity by anchoring the E2 to the HECT domain. *Mol Cell* **19:** 297–308

Oliver PM, Cao X, Worthen GS, Shi P, Briones N, MacLeod M, White J, Kirby P, Kappler J, Marrack P, Yang B (2006) Ndfip1 protein promotes the function of itch ubiquitin ligase to prevent T cell activation and T helper 2 cell-mediated inflammation. *Immunity* **25:** 929–940

Rotin D, Kumar S (2009) Physiological functions of the HECT family of ubiquitin ligases. *Nat Rev Mol Cell Biol* **10:** 398–409

Robu ME, Larson JD, Nasevicius A, Beiraghi S, Brenner C, Farber SA, Ekker SC (2007) p53 activation by knockdown technologies. *PLoS Genet* **3:** e78

Salahudeen AA, Thompson JW, Ruiz JC, Ma HW, Kinch LN, Li Q, Grishin NV, Bruick RK (2009) An E3 ligase possessing an iron-responsive hemerythrin domain is a regulator of iron homeostasis. *Science* **326:** 722–726

Sapkota G, Alarcon C, Spagnoli FM, Brivanlou AH, Massague J (2007) Balancing BMP signaling through integrated inputs into the Smad1 linker. *Mol Cell* **25:** 441–454

Skaar JR, D'Angiolella V, Pagan JK, Pagano M (2009a) SnapShot: F box proteins II. *Cell* **137:** 1358, 1358.e1

Skaar JR, Pagan JK, Pagano M (2009b) SnapShot: F box proteins I. *Cell* **137:** 1160, e1160.e1

Subramaniam V, Li H, Wong M, Kitching R, Attisano L, Wrana J, Zubovits J, Burger AM, Seth A (2003) The RING-H2 protein RNF11 is overexpressed in breast cancer and is a target of Smurf2 E3 ligase. *Br J Cancer* **89:** 1538–1544

Suzuki A, Shibata T, Shimada Y, Murakami Y, Horii A, Shiratori K, Hirohashi S, Inazawa J, Imoto I (2008) Identification of SMURF1 as a possible target for 7q21.3-22.1 amplification detected in a pancreatic cancer cell line by in-house array-based comparative genomic hybridization. *Cancer Sci* **99:** 986–994

Wang HR, Zhang Y, Ozdamar B, Ogunjimi AA, Alexandrova E, Thomsen GH, Wrana JL (2003) Regulation of cell polarity and protrusion formation by targeting RhoA for degradation. *Science* **302:** 1775–1779

Wiesner S, Ogunjimi AA, Wang HR, Rotin D, Sicheri F, Wrana JL, Forman-Kay JD (2007) Autoinhibition of the HECT-type ubiquitin ligase Smurf2 through its C2 domain. *Cell* **130:** 651–662

Xia L, Jia S, Huang S, Wang H, Zhu Y, Mu Y, Kan L, Zheng W, Wu D, Li X, Sun Q, Meng A, Chen D (2010) The Fused/Smurf complex controls the fate of Drosophila germline stem cells by generating a gradient BMP response. *Cell* **143:** 978–990

Yamashita M, Ying SX, Zhang GM, Li C, Cheng SY, Deng CX, Zhang YE (2005) Ubiquitin ligase Smurf1 controls osteoblast activity and bone homeostasis by targeting MEKK2 for degradation. *Cell* **121:** 101–113

Zhao L, Huang J, Guo R, Wang Y, Chen D, Xing L (2010) Smurf1 inhibits mesenchymal stem cell proliferation and differentiation into osteoblasts through JunB degradation. *J Bone Miner Res* **25:** 1246–1256

Zhao M, Qiao M, Oyajobi BO, Mundy GR, Chen D (2003) E3 ubiquitin ligase Smurf1 mediates core-binding factor alpha1/Runx2 degradation and plays a specific role in osteoblast differentiation. *J Biol Chem* **278:** 27939–27944

Zhu H, Kavsak P, Abdollah S, Wrana JL, Thomsen GH (1999) A SMAD ubiquitin ligase targets the BMP pathway and affects embryonic pattern formation. *Nature* **400:** 687–693